Bioorganic & Medicinal Chemistry 22 (2014) 3931–3937

Contents lists available at ScienceDirect

Bioorganic & Medicinal Chemistry

journal homepage: www.elsevier.com/locate/bmc

Synthesis and evaluation of the novel 2-[^{18}F]fluoro -3-propoxy-triazole-pyridine-substituted losartan for imaging AT_1 receptors

Natasha Arksey [a,b], Tayebeh Hadizad [a], Basma Ismail [a,b], Maryam Hachem [a,b], Ana C. Valdivia [a,b], Rob S. Beanlands [a,b], Robert A. deKemp [a], Jean N. DaSilva [a,b,c,*]

[a] Cardiac PET Centre, University of Ottawa Heart Institute, 40 Ruskin St., Ottawa, ON, Canada
[b] Department of Cellular and Molecular Medicine, University of Ottawa, Ottawa, ON, Canada
[c] Department of Radiology, Radio-Oncology and Nuclear Medicine, University of Montreal, University of Montreal Hospital Research Centre (CRCHUM), Montréal, Québec, Canada

ARTICLE INFO

Article history:
Received 26 February 2014
Revised 28 May 2014
Accepted 6 June 2014
Available online 17 June 2014

Keywords:
Fluorine-18
Click chemistry
Losartan
FPyKYNE
AT_1
PET

ABSTRACT

The 2-[^{18}F]fluoro-3-pent-4-yn-1-yloxypyridine ([^{18}F]FPyKYNE) analog of the potent non-peptide angiotensin II type 1 receptor (AT_1R) blocker losartan was produced via click chemistry linking [^{18}F]FPyKYNE to azide-modified tetrazole-protected losartan followed by TFA deprotection. Preliminary small animal imaging with positron emission tomography (PET) in rats displayed high uptake in the kidneys with good contrast to surrounding tissue. Rat metabolism displayed the presence of 23% unchanged tracer in plasma at 30 min. Upon co-administration with AT_1R blocker candesartan (2.5, 5 and 10 mg/kg), a dose-dependent reduction (47–65%) in tracer uptake was observed in the kidney, while no difference was observed following AT_2R blocker PD123,319 (5 mg/kg), indicating binding selectivity for AT_1R over AT_2R and potential for imaging AT_1R using PET.

1. Introduction

The renin-angiotensin-system (RAS) is an important regulator of blood pressure and exerts its effects mainly through activation of the AT_1R and AT_2R subtypes by angiotensin II. Activation of the AT_1R induces most of the known pathophysiologic effects of angiotensin II, including vasoconstriction, sodium and water retention, hypertrophy, cell proliferation and fibrosis.[1] In addition to angiotensin-converting enzyme inhibitors, AT_1R blockers such as losartan, are well established therapies for the treatment of hypertension and cardiovascular diseases. Several diseases including renal hypertension, diabetes and myocardial infarction exhibit AT_1R dysregulation. The ability to non-invasively detect this abnormal regulation by molecular imaging modalities such as PET provides the potential to monitor disease progression and guide therapy accordingly.

Previous AT_1R PET tracers have been labeled with C-11,[2–4] however F-18 offers some key advantages: namely, a longer half-life (109.6 vs 20.4 min)[5] allowing for multiple patient scans from a single formulation and shipment to other sites without radiochemistry or cyclotron capabilities, and a shorter RMS (Root Mean Squared) positron range (0.23 vs 0.39 mm in soft tissue)[6] enabling higher resolution images. Structure–activity relationship studies and recent work reported that large prosthetic groups can be introduced at the imidazole 5-position with minimal changes both in binding properties and antagonistic efficacy compared to the parent compound.[2,7]

Click chemistry[8] is a popular method of conjugation, owing to the regiospecific nature of the reactions, mild reaction conditions, high yields and ease of purification. The mainstay of click chemistry is the copper(I)-catalyzed azide-alkyne cycloaddition (CuAAC).[9] This ligation is one of only a few truly chemoselective and regioselective reactions. The resulting linkage, a 1,4-disubstituted triazole, acts as amide bond isostere, but is more resistant to hydrolysis, oxidation and reduction in physiological conditions.[10] Several ^{18}F-labeled alkynes and their subsequent use in click chemistry have been described in the literature.[11,12]

Herein we describe the conjugation of [^{18}F]FPyKYNE, following the procedure already published,[13] to azide-modified trityl losartan

* Corresponding author. Addresses: Department of Radiology, Radio-Oncology and Nuclear Medicine, University of Montreal. CRCHUM - Tour Viger, 900 rue St-Denis, Room R11.440, Montréal, QC H2X 0A9, Canada. Tel.: +1 (514)890 8000x30653.
E-mail address: jean.dasilva@umontreal.ca (J.N. DaSilva).

http://dx.doi.org/10.1016/j.bmc.2014.06.011
0968-0896/

via click chemistry using an automated dual reactor module (TRACERlab FX N Pro) and provide a preliminary in vivo evaluation of the novel ^{18}F-labeled losartan derivative in rats using micro-PET imaging. To the best of our knowledge, there are currently no publications describing the synthesis of an F-18 labeled AT_1R PET tracer.

2. Results and discussion

2.1. Chemistry

The synthesis of 2-butyl-4-chloro-5-[[3-{[1-methyl-4-yl](1,2,3) triazol}propoxy]-2-fluoro-pyridine]-1-[[2′-[tetrazole-5-yl]biphenyl-4-yl]methyl]imidazol, **5a**, hereafter named FPyKYNE-losartan, is described in Scheme 1. It's precursor, 2-butyl-4-chloro-5-(azido methyl)-1-[[2′-[(triphenylmethyl)tetrazole-5-yl]biphenyl-4-yl] methyl]imidazol **4,** was prepared according to the method previously reported,[14] a nucleophilic substitution reaction that converts the 5′ hydroxymethyl group in **3** to the corresponding azide moiety in 87% yield. Compound **1**, NO_2PyKYNE (2-nitro-3-pent-4-yn-1-yloxypyridine), **2a** FPyKYNE (2-fluoro-3-pent-4-yn-1-yloxypyridine) and **2b** [^{18}F]FPyKYNE were synthesized according to the literature.[15,16] Replacement of the nitro group on **1** by fluorine using potassium fluoride (KF) readily afforded the cold prosthetic group **2a**. Both compounds **1** and **2a** were characterized by ^{1}H and ^{13}C NMR and high-resolution mass spectrometry (HRMS). Compound **2a** was further characterized by ^{19}F NMR. The results proved consistent with those reported.[15] Cyclocondensation of **2a** and **4** was achieved through the copper(I)-catalyzed cycloaddition reaction using an aqueous solution of copper(II) sulfate ($CuSO_4$) and sodium ascorbate as the source of Cu(I). The reaction was amenable to a range of temperatures (room temperature to 120 °C) and a variety of co-solvents (e.g., DMSO, DMF, CH_2Cl_2, MeCN). A quick acid hydrolysis of the protected tetrazole with TFA at 80 °C followed by flash column chromatography purification afforded the desired product **5a**, FPyKYNE-losartan, in 44% yield. Compound **5a** was fully characterized by accurate mass measurement, ^{1}H NMR, ^{13}C NMR, and ^{19}F NMR.

2.2. Radiochemistry

The first step in the production of [^{18}F]FPyKYNE-losartan, **5b** was radiofluorination of the nitro precursor **1** (Scheme 1). This step occurred in the first reaction vessel of the TRACERlab FX N Pro using [^{18}F]KF/K_{222}/K_2CO_3 in anhydrous DMSO at 120 °C for 10 min. Purified **2b** was delivered to the second reaction vessel in a 15–20% yield (decay-corrected) by passing the reaction mixture through a series of three silica cartridges with an eluent of 50:50 ether/pentane.[16] Following evaporation of the solvent, the labeled prosthetic group **2b** was then conjugated to the azide-modified tetrazole-protected losartan precursor **4** for 30 min at 95 °C in DMSO. The reaction mixture was then cooled, treated with TFA, and heated to 80 °C for 2 min prior to loading onto HPLC. The fraction containing **5b** was collected and loaded onto a preconditioned C18 cartridge (SPE) to remove the HPLC solvents. Pure **5b** was eluted with minimal EtOH and diluted in saline to provide the final product in 44–70% yield (decay-corrected from **2b**), or an overall yield of 7–14% (decay-corrected from end-of-beam (EOB)). The yield is much lower than that of the non-radioactive synthesis likely due to shorter reaction times, the amount of F-18 fluoride available for radiofluorination compared to the stoichiometric quantities used for the synthesis of the standard, and product loss in the components of the module (i.e., reaction vessels, tubing, SPE cartridges).

The identity of the product was confirmed by a single peak on analytical HPLC following a co-injection of the formulated product with cold standard (Fig. 1). The radiochemical purity was consistently greater than 98% with specific activity from 200–4200 mCi/μmol (7.4–155 GBq/μmol). The entire synthesis, including reformulation, took less than 2 h from EOB. In a representative synthesis, 40 mCi (1.48 GBq) of labeled product **5b** could be obtained from 850 mCi (31.45 GBq) of [^{18}F]fluoride.

The level of copper in the final formulations measured by inductively coupled plasma (ICP) MS was 23.3 ± 5.4 ppb, 26.3 ± 6.5 ppb in blanks, 23.6 ppb in pure saline, and 18 ppb in pure ethanol, all well below the pharmaceutically maximum acceptable exposure to residual metals on a chronic basis. These results indicate no meaningful contamination of copper in the final formulation.

2.3. Biological evaluation in rats

Preliminary in vivo evaluation of the binding properties of [^{18}F]FPyKYNE-losartan was performed using micro-PET imaging. Normal untreated rats showed the greatest accumulation of activity in the liver and kidneys, respectively (Fig. 2A). The time-activity curves (TAC) derived from the left kidney displayed a sharp increase in activity uptake in the first few minutes, following the arterial blood input functions, which then washed out slowly to background levels around 55 min (Fig. 2B). The renal activity had

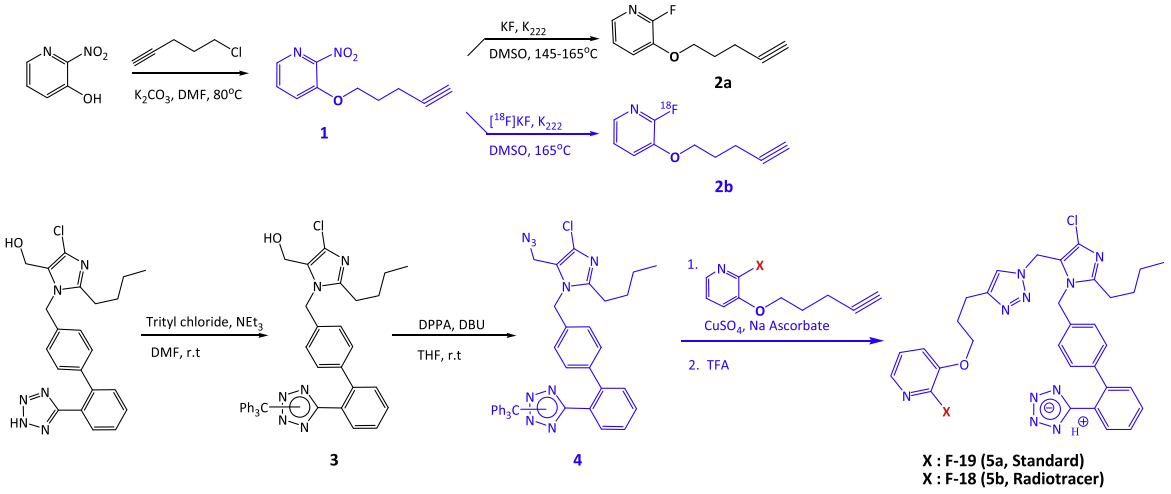

Scheme 1. Synthesis of [^{18}F]FPyKYNE-losartan and standard via the Cu(I)-catalyzed [2 + 3] cycloaddition reaction between azide-modified losartan and [^{18}F]FPyKYNE, performed in the TRACERlab FX_{F-N} automated module (GE Healthcare).

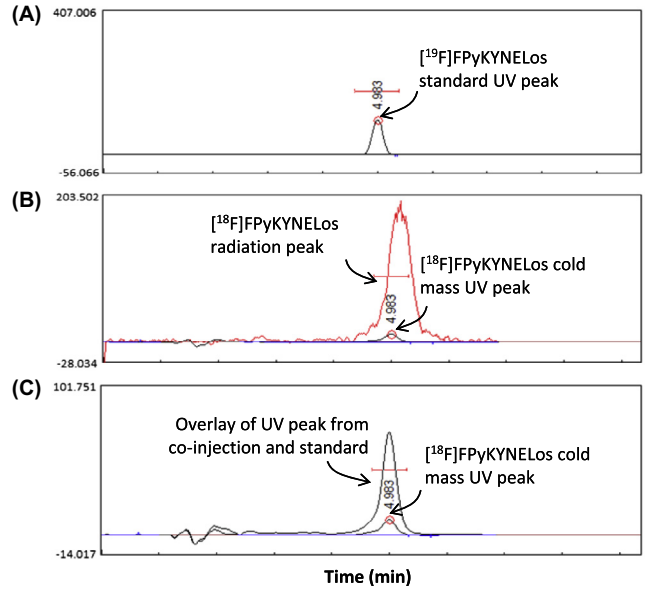

Figure 1. Quality control for [^{18}F]FPyKYNE-losartan formulated product by analytical HPLC. (A) UV chromatogram of cold standard; (B) radiation and UV chromatogram of product formulation; (C) UV chromatogram from co-injection of product and standard overlaid on UV chromatogram of product from B. UV spectra were recorded at 254 nm. Column: Phenomenex Luna C18(2) (10 μM, 250 × 4.6 mm) with 40:60 MeCN/AF (0.1 M) at 2 mL/min; PeakSimple 3.93 Analysis Software.

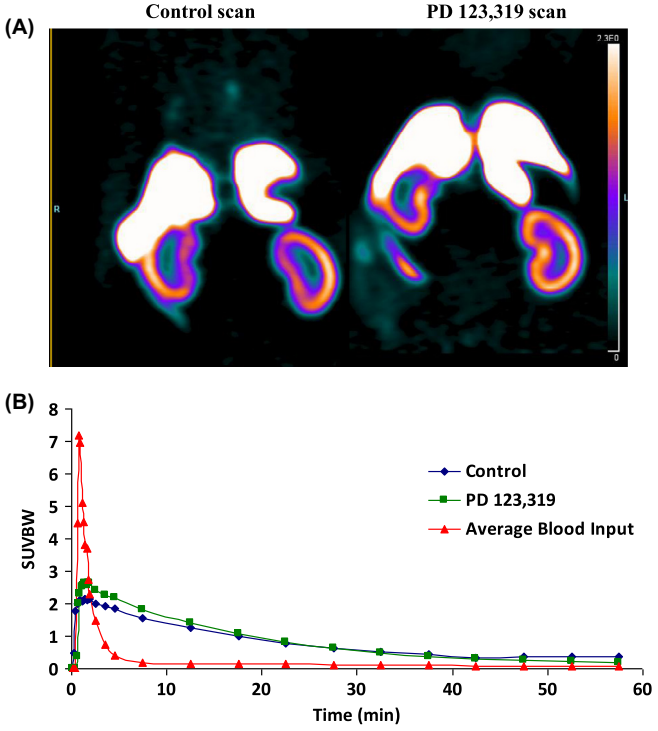

Figure 2. Representative microPET images (coronal view) of [^{18}F]FPyKYNE-losartan showing liver and kidney activity (specific uptake values) at 5-10 min post-injection in (A) normal animals (n = 7) and AT_2R blocked animals with 5 mg/kg PD 123,319 (n = 3). (B) Tracer time-activity curves for average blood input (left atrium) and kidney are presented as specific uptake values normalized to body weight (SUV_{BW}) from 0 to 60 min.

a specific uptake value (SUV) of 1.52 ± 0.58 at 10 min post-injection. Using Logan graphical analysis of image-derived renal versus left atrium blood TAC, the average distribution volume (DV) of [^{18}F]FPyKYNE-losartan in the left kidney was 2.76 ± 0.68 mL/cm^3.

2.3.1. In vivo competition studies

In rats treated with the AT_2R antagonist PD 123,319 (IC_{50} for rat adrenal AT_2R = 34 nM),[17] kidney TAC followed similar time course to normal rats (Fig. 2). No effect on tracer binding to AT_1R was observed (DV values were 2.76 ± 0.68 and 3.02 ± 0.20 (p = 0.28) for normal and PD 123,319 blocking scans, respectively) confirming [^{18}F]FPyKYNE-losartan binding selectivity for AT_1R over AT_2R.

A significant 47–65% (p <0.02) dose-dependent reduction in renal uptake of the tracer was observed after administration of candesartan (IC_{50} for AT_1R = 110 nM),[18] suggesting AT_1R binding specificity. Doses of 2.5, 5.0, and 10 mg/kg reduced the SUV at 10 min to 1.25 ± 0.17, 0.99 ± 0.38 and 0.61 ± 0.15, respectively. Similarly, the DV values were reduced in a dose-dependent manner to 1.46 ± 0.30, 1.45 ± 0.21 and 0.96 ± 0.06 mL/cm^3 with doses of 2.5, 5 and 10 mg/kg, respectively (Fig. 3).

2.3.2. Radiolabeled metabolite analysis of [^{18}F]FPyKYNE-losartan in rat plasma

Column-switch High Performance Liquid Chromatography (HPLC) metabolite analysis of [^{18}F]FPyKYNE-losartan exhibited three distinct radioactive peaks in rat plasma, with retention times of approximately 0.5–1 min (peak 1), 6.8 min (peak 2) and 10 min (peak 3) post-switch, respectively (Fig. 4). Peak 1 corresponds to hydrophilic labeled metabolite(s) eluted from the capture column, that is unlikely to bind to AT_1R. Peak 2 is a hydrophobic labeled metabolite that can potentially bind to AT_1R, and peak 3 represents unchanged tracer. At 30 min after injection, 78 ± 10% of total radioactivity (noise- and decay-corrected) was from peak 1, 1 ± 1% peak 2, and 23 ± 10% was unchanged [^{18}F]FPyKYNE-losartan (Fig. 5). In control plasma samples, radioactivity present was solely representative of unchanged [^{18}F]FPyKYNE-losartan (data not shown).

3. Conclusions

Radiosynthesis of [^{18}F]FPyKYNE-losartan has been achieved in high radiochemical purity and acceptable specific activity for renal imaging. The production method was reliable, providing sufficient amount of tracer, with no meaningful copper contamination, for multiple PET scans. [^{18}F]FPyKYNE-losartan PET images obtained in rats displayed high tissue contrast and binding selectivity for renal AT_1R over AT_2R. [^{18}F]FPyKYNE-losartan metabolism to mostly hydrophilic labeled compounds in plasma suggests minimal interference of ^{18}F-labeled metabolites to AT_1Rs. These findings support the use of this tracer for renal AT_1R evaluation with non-invasive imaging in rats.

4. Experimental section

4.1. Materials and methods

Reaction solvents, including MeCN and DMSO as well as purification solvents (pentane and diethyl ether) were anhydrous (>99%) ACS grade by Sigma–Aldrich. HPLC grade MeCN was purchased from Fisher Scientific, Trifluoroacetic acid (TFA, 99%) from Alfa Aesar and losartan potassium (98%) from LKT Laboratories, Inc (Medicorp, Montreal, QC). All other reagents, including deuterated solvents for NMR, were purchased from Sigma–Aldrich and classified as 98% purity or greater. EtOH (99.9%) and saline solution (0.9%) for reformulation were obtained from sterile capped bottles. No further manipulation or purification was made to purchased solvents and/or reagents.

Analytical TLC was performed on silica gel-coated aluminum sheets (Sigma–Aldrich). Unless specified otherwise, TLC was run with a solvent of 30:70 EtOAc/Hexanes. Preparative TLC was performed on Analtech TLC Uniplates (silica gel matrix, 1000 μM). A

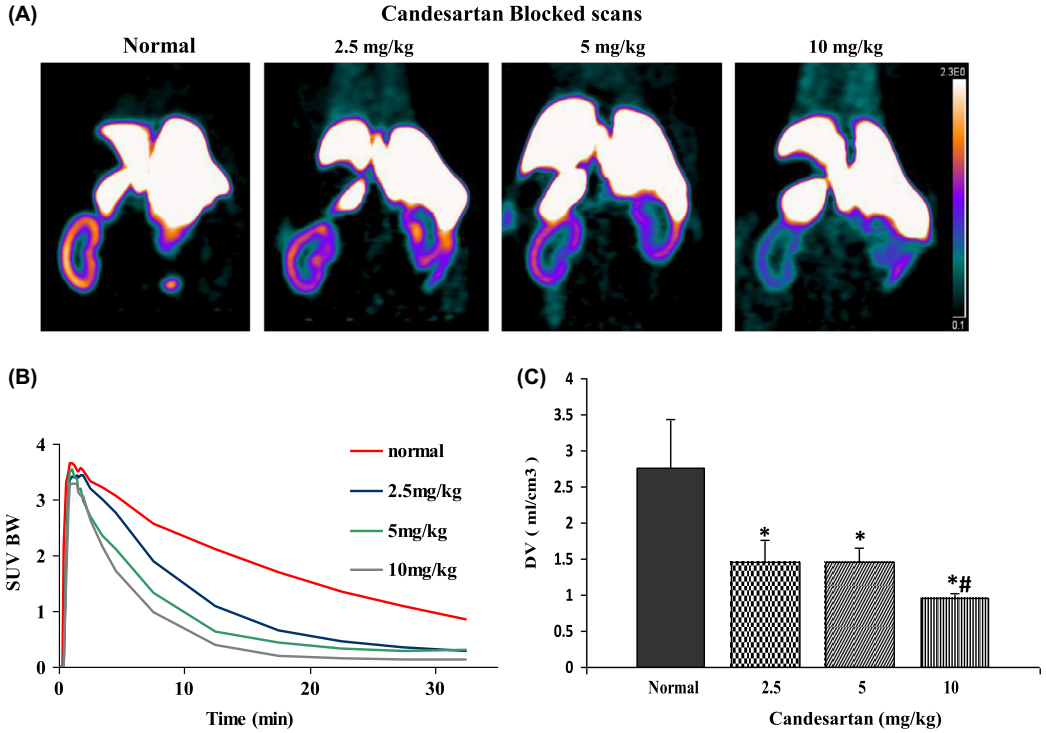

Figure 3. (A) MicroPET images (coronal view) of [^{18}F]FPyKYNE-losartan showing liver and kidney activity (specific uptake values) at 10–15 min post-injection. Effect of AT_1R blocking with increasing candesartan doses (2.5 mg/kg, $n = 3$; 5 mg/kg, $n = 5$; and 10 mg/kg, $n = 3$) on (B) specific uptake value (SUV) time-activity curves from 0 to 60 min, and (C) distribution volume (DV) of [^{18}F]FPyKYNE-losartan determined by Logan analysis in the kidney of rats. $^{*}P$ <0.02 compared to baseline; $^{\#}P$ <0.02 compared to previous dose.

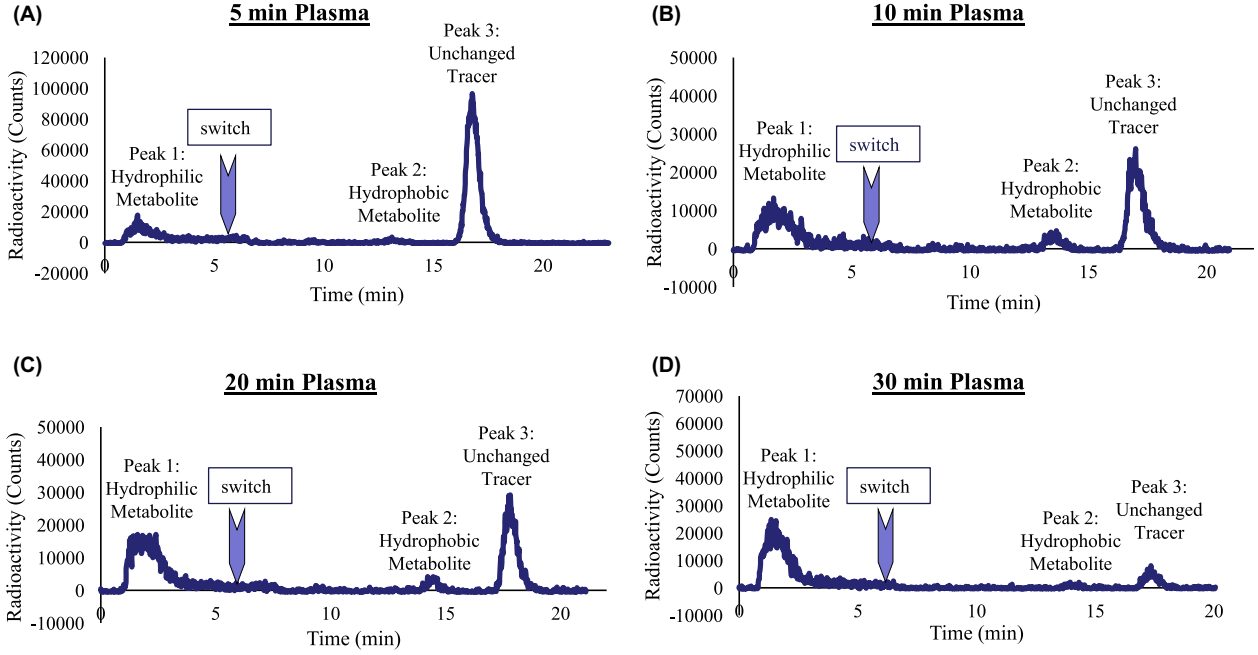

Figure 4. Representative HPLC chromatograms displaying presence of unchanged [^{18}F]FPyKYNE-losartan and its labeled metabolites, in rat plasma at respective time points. [^{18}F]FPyKYNE-losartan (peak 3) is metabolized into a hydrophilic metabolite (peak 1) and a hydrophobic metabolite (peak 2). Plasma samples were analyzed at 5 min (A), 10 min (B), 20 min (C) and 30 min (D) post tracer injection.

technical grade silica gel (Davisil® grade 633, 60 Å pore size, 200–425 mesh) purchased from Sigma–Aldrich was used for flash column chromatography. A Phenomenex Luna C18(2) column (250 × 4.6 mm, 10 μM) was used for all analytical HPLC and a Phenomenex® Luna C18(2) column (250 × 10 mm, 10 μM) was installed in the module for HPLC purification. PeakSimple Chromatography Data System (6-port) was used in combination with a Waters 486 Tunable Absorbance Detector and Water 515 HPLC Pump and data analysed by PeakSimple (v 3.93). Sep-Pak Light Waters Accell Plus QMA cartridges and Sep-Pak Light C18

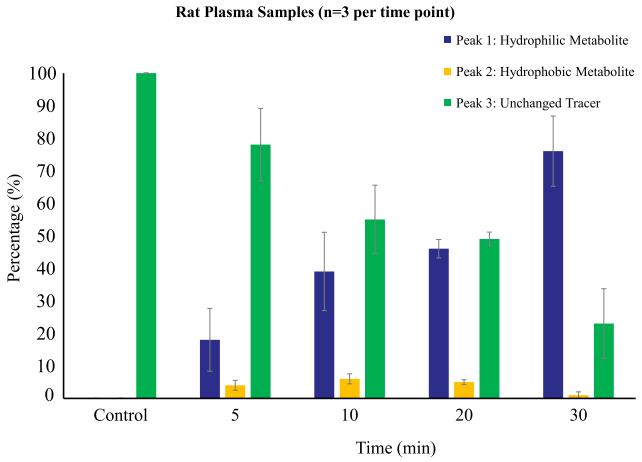

Figure 5. Proportions of [^{18}F]FPyKYNE-losartan and its labeled metabolites in rat plasma over time. In the control sample, 100% of radioactivity represents unchanged tracer. From 5 to 30 min unchanged [^{18}F]FPyKYNE-losartan is rapidly metabolized and reduced from 78% to 23%, respectively.

cartridges for SPE were purchased from Waters. The QMA cartridges were conditioned by passing through 7–8 mL of a 0.55 M solution of potassium carbonate (7.60 g or 0.055 mol K_2CO_3 in 100 mL water), followed by water (7–8 mL) and drying under a stream of argon. The C18 cartridges were pre-conditioned by passing through 5 mL of EtOH followed by 10 mL of water. Silica cartridges were used as received. F-18 eluent was prepared by dissolving 27.5 mg (0.20 mmol) K_2CO_3 and 150 mg (0.40 mmol) Kryptofix2.2.2 (K_{222}) in a 5 mL solution of MeCN (4.75 mL) and water (250 μl). Melting points (Mp) were measured by a Fisher Scientific melting point apparatus.

NMR, HRMS, Accurate Mass Measurement and ICP MS were performed at the University of Ottawa. ^{1}H NMR was carried out in $CDCl_3$, unless otherwise indicated either by a Bruker AVANCE 300 or 400 MHz, or a Varian Inova 500 MHz spectrometer. ^{13}C NMR and ^{19}F NMR spectra were obtained on a Bruker AVANCE 300 MHz spectrometer. Proton chemical shifts (δ) are reported in parts per million (ppm) relative to tetramethylsilane (TMS) internal standard. Coupling constants (J) are reported in Hz. HRMS were done on either a Concept HRes, EI Mass Spectrometer or a Micromass QToF, ESI HRes Mass Spectrometer (for accurate mass measurement). ICP MS was performed on a Varian (Agilent) Vista-Pro Inductively coupled plasma emission spectrometer, equipped with a charge-coupled device (CCD) detector.

[^{18}F]F$^-$ was produced in a CTI/Siemens RDS III cyclotron by proton irradiation of [^{18}O]H_2O (>97%) via the ^{18}O(p,n)^{18}F nuclear reaction. The TRACERlab FX N Pro automated synthesizer, including UV detector, HPLC pump, and software, were purchased from GE Healthcare. Radioactivity was measured in a Capintec dose calibrator.

4.2. Chemistry

4.2.1. 2-Nitro-3-pent-4-yn-1-yloxypyridine (NO_2PyKYNE, 1)

Compound **1** was synthesized according to the literature.[15] A solution containing 2-nitro-3-hydroxypyridine, potassium carbonate (K_2CO_3), sodium iodide (NaI) and 5-chloropent-1-yne in DMF was stirred overnight at 80 °C. The reaction mixture was cooled and diluted with EtOAc for extraction with water and brine. After drying over Na_2SO_4, the solvent was removed under reduced pressure and the residue purified by flash column chromatography on silica gel (85:15 Hexane/EtOAc) to afford **1** as a white crystalline powder. Mp 56–58 °C. HPLC [50:50 MeCN/H_2O (0.1 M AF), 2 mL/min]: 4.6 min. ^{1}H NMR (300 MHz, $CDCl_3$) δ_H 8.08 (dd, J = 3.2, 2.6 Hz, 1H); 7.51–7.50 (m, 2H); 4.23 (t, J = 6.0 Hz, 2H); 2.45 (td, J = 6.8, 2.6 Hz, 2H); 2.03 (qn, J = 6.1 Hz, 2H); 1.95 (t, J = 2.6 Hz, 1H). ^{13}C NMR (75 MHz, $CDCl_3$) δ_C 150 (C); 147.14 (C); 139.20 (CH); 128.53 (CH); 123.43 (CH); 82.68 (C); 69.43 (CH); 67.88 (CH_2); 27.58 (CH_2); 14.87 (CH_2). HRMS: calcd for $C_{10}H_{10}N_2O_3$ [M+H]$^+$, 207.0677, found 207.0323. The ^{1}H and ^{13}C NMR as well as HRMS data confirmed product identity and were in agreement with the reported values.

4.2.2. 2-Fluoro-3-pent-4-yn-1-yloxypyridine (FPyKYNE, 2a)

As described previously,[15] compound **2a** was synthesized by reacting NO_2PyKYNE **1** with potassium fluoride and Kryptofix2.2.2 in DMSO at 145–165 °C for 90 min. The reaction was monitored for completion by TLC. After cooling to room temperature, the reaction mixture was diluted with EtOAc and extracted with water and brine then dried over Na_2SO_4 before removing the solvent under reduced pressure. The residue was purified by flash column chromatography on silica gel (85:15 Hexanes/EtOAc) to afford **2a** as clear crystalline oil. HPLC [50:50 MeCN/H_2O (0.1 M AF), 2 mL/min]: 4.6 min. ^{1}H NMR (300 MHz, $CDCl_3$) δ_H 7.75 (dd, J = 4.8, 1.6 Hz, 1H); 7.32 (m, 1H); 7.12 (dd, J = 7.8, 4.9 Hz, 1H); 4.17 (t, J = 6.1 Hz, 2H); 2.45 (td, J = 6.9, 2.6 Hz, 2H); 2.05 (qn, J = 6.4 Hz, 2H); 2.0 (t, J = 2.6 Hz, 1H). ^{13}C NMR (75 MHz, $CDCl_3$) δ_C 153.85 (C, J^1_{C-F} = 237.3 Hz); δ: 142.23 (C, J^2_{C-F} = 25.4 Hz); 137.37 (C, J^3_{C-F} = 13.2 Hz); δ: 122.81 (C, J^3_{C-F} = 4.4 Hz); δ: 121.66 (C, J^4_{C-F} = 4.3 Hz); 82.93 (C); 69.16 (CH); 67.50 (CH_2); 27.83 (CH_2); 14.96 (CH_2). ^{19}F NMR δ_F −84.79 (referenced with respect to TFA). HRMS: calcd for $C_{10}H_{10}FNO$ [M+H]$^+$, 180.0732, found 180.0443.

4.2.3. 2-Butyl-4-chloro-5-(hydroxymethyl)-1-[[2′-[(triphenylmethyl)tetrazole-5-yl]biphenyl-4-yl]methyl]imidazol (tetrazole-protected losartan, 3)

Compound **3** was prepared from commercially available losartan potassium as previously described.[2] Briefly, to a solution of losartan in DMF was added trityl chloride and Et_3N. The solution was stirred at room temperature overnight after which it was diluted with EtOAc, washed with water and brine, dried over Na_2SO_4 and solvent removed. The residue was purified by flash column chromatography on silica gel to obtain a white powder. HPLC [35:65 MeCN/AF (0.1 M), 2 mL/min]: 3.6 min. ^{1}H NMR (400 MHz, DMSO-d_6) δ_H 7.79 (d, J = 6.0 Hz, 1H); 7.61 (t, J = 6.0 Hz, 1H); 7.54 (t, J = 6.0 Hz, 1H); 7.31–7.44 (m, 10H); 7.05 (d, J = 6.4 Hz, 2H); 6.90 (d, J = 6.4 Hz, 2H); 6.86 (d, J = 6.0 Hz, 6H); 5.24 (t, J = 4.0 Hz, 1H); 5.19 (s, 2H); 4.21 (d, J = 4.0 Hz, 2H); 2.37 (t, J = 6.0 Hz, 2H); 1.41 (q, J = 6.0 Hz, 2H); 1.15 (sx, J = 6.0 Hz, 2H); 0.73 (t, J = 6.0 Hz, 3H). HRMS: calcd for $C_{41}H_{37}ClN_6O$ [M+Na], 687.2615, found 687.2638.

4.2.4. 2-Butyl-4-chloro-5-(azidomethyl)-1-[[2′-[(triphenylmethyl)tetrazole-5-yl]biphenyl-4-yl]methyl]imidazol (tetrazole-protected azido-losartan, 4)

To a solution of **3** (300 mg, 0.44 mmol) in THF (4 mL) were added 18-diazabicyclo[5.4.0]-7-undecene (DBU, 74 mg, 0.48 mmol) and diphenylphosphoryl azide (DPPA, 105 μl, 0.49 mmol). The reaction mixture was stirred at ambient temperature under argon for overnight (16 h) and monitored by TLC for completion. The reaction was then quenched with water (2 mL). The organic phase was separated, and the aqueous phase extracted with EtOAc. The organic phases were combined and dried over Na_2SO_4. The solvent was removed under reduced pressure and the residue purified by flash column chromatography (EtOAc/Hexanes 5:95–30:70) to afford **4** (275 mg, 87%) as a white crystalline powder. Mp 130–132 °C. ^{1}H NMR (300 MHz, $CDCl_3$) δ_H 7.96 (m, 1H); 7.41-7.51 (m, 2H); 7.30-7.36 (m, 10H); 7.11 (d, J = 8.2 Hz, 2H); 6.90 (d, J = 7.7 Hz, 2H); 6.70 (d, J = 8.2 Hz, 6H); 4.98 (s, 2H); 3.94

(s, 2H); 2.51 (t, J = 7.8 Hz, 2H); 1.66 (qn, J = 7.7 Hz, 2H); 1.29 (sx, J = 7.4 Hz, 2H); 0.86 (t, J = 7.3 Hz, 3H). ^{13}C NMR (75 MHz, $CDCl_3$) δ_C 149.42 (C); 146.80 (C); 145.20 (3 × C); 141.23 (C); 130.61 (3 × C); 129.64 (C); 128.40 (7 × CH); 127.90 (9 × CH); 127.6 (4 × CH); 126.99 (3 × CH); 125.31 (C); 77.24 (C); 42.14 (CH_2); 29.91 (CH_2); 29.67 (CH_2); 22.29 (CH_2); 22.23 (CH_2); 13.46 (CH_3). HRMS: calcd for $C_{41}H_{36}ClN_9$ [M+Na], 712.2680, found 712.2664.

4.2.5. 2-Butyl-4-chloro-5-[[3-{[1-methyl-4-yl](1,2,3)triazol}propoxy]-2-fluoro-pyridine]-1-[[2′-[tetrazole-5-yl]biphenyl-4-yl]methyl]imidazol (FPyKYNE-losartan, 5a)

To a stirred solution of tetrzol-protected azido-losartan **4** (50 mg, 0.072 mmol) in CH_2Cl_2 (1.5 mL) was added a solution of FPyKYNE, **2a** (14.28 mg, 0.080 mmol) in CH_2Cl_2 (400 μl) followed by aqueous solutions of copper(II) sulfate ($CuSO_4$, 50 μl, 0.06 M) and sodium ascorbate (120 μl, 0.05 M). The biphasic solution was stirred at ambient temperature overnight (16 h). The reaction was monitored by TLC for completion after which it was diluted with EtOAc and extracted with water (2 × 30 mL) and brine (30 mL) then dried over Na_2SO_4 before removing the solvent under reduced pressure. The residue was diluted with a solution of TFA in DMF (400 μl, 0.13 mM) and heated at 80–85 °C for 1–2 min. The product was purified by semi-prep TLC (silica on glass, EtOAc/Hexanes/MeOH 80:20:5) to obtain **5a** (20 mg, 44%) as a clear oil which was then crystallized with chloroform to yield a white solid. Mp 162–165 °C. ^{1}H NMR (300 MHz, $CDCl_3$) δ_H 7.86 (dd, J = 7.51, 1.4 Hz, 1H); 7.65-7.68 (m, 1H); 7.52 (td, J = 7.47, 1.6 Hz, 1H); 7.46 (td, J = 7.53, 1.7 Hz, 1H); 7.24–7.36 (m, 1H); 6.98-7.07 (m,4H); 6.81 (d, J = 8.4 Hz, 2H); 6.39 (d, J = 8.3 Hz, 2H); 5.40–5.24 (m, 4H); 3.81 (t, J = 6.3 Hz, 2H); 2.60 (t, J = 7.8 Hz, 4H); 1.86 (qn, J = 6.7 Hz, 2H); 1.67 (qn, J = 7.7 Hz, 2H); 1.34 (sx, J = 7.5 Hz, 2H); 0.86 (t, J = 7.3 Hz, 3H). ^{19}F NMR (referenced with respect to TFA) δ_F −84.88 (d, J = 8.78 Hz). ^{13}C NMR (75 MHz, $CDCl_3$) δ_C 153.75 (C); 152.17 (C); 150.15 (C); 147.29 (C); 142.03 (C); 139.97 (C); 138.30 (C); 137.56 (C); 135.16 (C); 131.89 (C); 131.55 (C); 130.47 (2 × CH); 130.06 (2 × CH); 129.46 (CH); 128.49 (CH); 124.65 (CH); 123.15 (CH); 122.85 (CH); 121.93 (CH); 120.64 (CH); 120.24 (CH); 67.83 (CH_2); 53.62 (CH_2); 47.34 (CH_2); 42.55 (CH_2); 29.93 (CH_2); 28.33 (CH_2); 26.89 (CH_2); 22.55 (CH_2); 13.85 (CH_3). HRMS: calcd for $C_{32}H_{32}ClFN_{10}O$ [M−H], 625.2355, found 625.2357.

4.3. Radiochemistry

4.3.1. 2-Butyl-4-chloro-5-[[3-{[1-methyl-4-yl](1,2,3)triazol}propoxy]-2-[^{18}F]fluoro-pyridine]-1-[[2′-[tetrazole-5-yl]biphenyl-4-yl]methyl]imidazol ([^{18}F]FPyKYNE-losartan, 5b)

The F-18 enriched target water was delivered to the module and loaded onto a QMA cartridge whereby F-18 was then eluted with an aqueous solution of potassium carbonate and Kryptofix2.2.2 (K_{222}) into the first reaction vessel. Azeotropic drying by evaporation of acetonitrile provided active un-solvated $K^+/K_{222}/^{18}F^-$. Nucleophilic substitution of the nitro group on NO_2PyKYNE **1** with F-18 produced [^{18}F]FPyKYNE **2b** which was then transferred to a series of three silica cartridges. The labeled product was eluted into the second reaction vessel and combined with tetrazole-protected azido-losartan **4** for conjugation. The product was deprotected with acid and sent to the semi-prep HPLC for purification. The collected fraction containing the product was then diluted with water and passed through a C-18 cartridge. After washing with water it was then eluted with EtOH (minimum value 0.4 mL) and reformulated in saline (maximum 10% EtOH solution).

4.3.2. Level of copper in the final formulation

The [^{18}F]FPyKYNE-losartan **5b**, was produced several times (n = 11) using different amounts of copper sulfate (1.5–2.25 mg, $9.4 \times 10^{-3} - 14.1 \times 10^{-3}$ mmol) and sodium ascorbate (3.25–4.9 mg, $16.4 \times 10^{-3} - 24.7 \times 10^{-3}$ mmol). The level of copper in the final formulations measured by ICP MS, was above the limit of detection (0.06 ppb), and the results were compared with blanks containing 10% ethanol in saline (prepared in different types of vials, n = 3), pure ethanol (n = 2) or pure saline (n = 1).

4.4. Animal studies

All experiments were performed with male Sprague Dawley rats weighing 200–660 g (Charles River Laboratories, Montreal, Canada) and were conducted in accordance with the guidelines of the Canadian Council of Animal Care (CCAC) and with approval from the Animal Care Committee (ACC) at the University of Ottawa. Rats were housed in pairs, kept on a 12 h light-dark cycle, and followed a standard diet.

4.4.1. In vivo microPET

Dynamic PET images were acquired with a Siemens Inveon small animal dedicated micro-PET scanner (LSO scintillation crystals, 1.4 mm spatial resolution, 12.7 cm axial FOV). Rats (n = 7) were anaesthetized with isoflurane (2–2.5%), weighed, and placed on the scanning bed in supine position with movement restricted by light taping. Anesthesia was maintained throughout the scanning process by a continuous flow of isoflurane (1–2%) through a nose cone. A slow-bolus of 0.4–1.0 mCi of [^{18}F]FPyKYNE-losartan was injected via a catheter in the lateral tail vein. List-mode data were acquired for 60 min and subsequently binned into 26 frames of 12 × 10 s, 3 × 60 s, and 11 × 300 s. Dynamic data were reconstructed on a 128 × 128 pixel image matrix (0.345 mm pixel size) using OSEM3D/MAP (β = 1.0, OSEM3D iterations = 2, MAP iterations = 18) with corrections for dead-time, isotope decay, detector efficiencies, attenuation, scatter and random events. A 10 min transmission scan with two rotating Co^{57} (122 keV) point sources was performed either prior to, or following the dynamic F-18 emission scan for attenuation correction.

In order to assess binding specificity for the AT_1R, subsets of rats (n = 3–5 per group) were co-injected with AT_1R blocker candesartan (2.5 mg/kg, 5 mg/kg and 10 mg/kg). Binding specificity for AT_2R[3,19] was examined in another rat group (n = 3) by injection of PD123,319 (5 mg/kg) 5 min prior to tracer injection.

4.4.2. Image analysis

Reconstructed dynamic images were analyzed using Siemens Inveon Research Workplace (IRW) software. TACs were generated for the arterial blood input function (derived from left atrium region of interest) and left kidney tissue uptake. [^{18}F]FPyKYNE-losartan renal activity was calculated as SUV (g/mL) at 5–10 min post-injection (frame 16). The SUV is a relative quantification of activity in a single or summed frame, normalized to the injected activity and the body weight of the rat, to allow comparison between subjects. Preliminary tracer binding was assessed by Logan graphical analysis.[20] Logan analysis is a graphical method used to quantify the tracer DV, which is the expected ratio of radiotracer in tissue relative to plasma at equilibrium for reversibly binding receptor ligands. The tracer DV (mL/cm^3) is an index of receptor density (B_{max}) and ligand affinity ($1/K_d$) for the receptor. Physiologically, the DV can be used as an indicator of protein expression and/or receptor-ligand binding potential (B_{max}/K_d) for reversibly binding ligands, that is, higher protein expression or binding affinity will result in a higher DV value.

4.4.3. Radiolabeled metabolite analysis in plasma

Restrained animals were injected with 2-4 mCi (74–148 MBq) [^{18}F]FPyKYNE-losartan via the lateral tail vein and sacrificed at −5 (control), 5, 10, 20 and 30 min post-injection (n = 3). Plasma

samples were prepared following centrifugation (4000×*g*, 5 min), by mixing with 1 g urea, to break binding with macromolecules, filtered through 0.2 μm syringe filters (Nylon Membrane, Acrodisc®), and injected onto the HPLC system. A modification of the HPLC column-switch method was used to quantify plasma metabolites.[21] Briefly, the HPLC apparatus consisted of 2 pumps (Waters): one eluting solvent A (1:99 MeCN/water [v/v]) at 1.5 mL/min across the capture cartridge (Alltech Direct-Connect refillable guard column, 2 × 20 mm) packed with sorbent (HLB VAC RC, Waters Oasis) and fitted with 2.5 μm frits (Alltech, 2-mm filter elements); and the other eluting solvent B (35:65 MeCN/0.1 M ammonium formate [v/v]) at 3 mL/min across the analytical column (Luna 10u C18 (2) 100A, 250 × 4.6 mm, 10 μm; Phenomenex). Eluents of both columns were analyzed in series by two detectors: the ultraviolet (UV) absorbance detector at 254 nm (Waters 486), and coincidence radiation detector (Bioscan). Signals were integrated using the PeakSimple Six-Port Chromatography Data System (Chromatographic Specialities), and expressed as the percentage of total noise- and decay-corrected radioactivity signal. Prepared samples (2 mL) were injected onto the capture column, then after elution of proteins, macromolecules and hydrophilic metabolites (6–7 min), column flow was switched delivering solvent B across the capture cartridge, eluting retained compounds onto the analytical column for analysis.

4.4.4. Statistical analysis

All results are expressed as mean ± standard deviation (SD). Statistical analyses were performed by a two-tailed *t*-test with a *p* value of less than 0.05 considered statistically significant.

Acknowledgments

The authors wish to thank the radiochemistry personnel, Yanick Lee and the Department of Chemistry of University of Ottawa for the chemistry. We would also like to extend our sincerest gratitude to Dr. Stephanie Thorn and Dr. James Thackeray for the help with the PET/bio-testing portion of this project. This work was supported in part by, the Ontario Preclinical Imaging Consortium (OPIC) Grant# RE03-51 (Ontario Research Foundation), the Heart and Stroke Foundation of Ontario Program Grant (PRG6242), and the Canadian Institutes of Health Research (MOP-287694).

Supplementary data

Supplementary data associated with this article can be found, in the online version, at http://dx.doi.org/10.1016/j.bmc.2014.06.011.

References and notes

1. Unger, T. *Am. J. Cardiol.* **2002**, *89*, 3A. discussion 10A.
2. Hadizad, T.; Collins, J.; Antoun, R. E.; Beanlands, R.; Dasilva, J. *J. Labelled Compd. Radiopharm* **2011**, *54*, 754.
3. Hadizad, T.; Kirkpatrick, S. A.; Mason, S.; Burns, K.; Beanlands, R. S.; Dasilva, J. N. *Bioorg. Med. Chem.* **2009**, *17*, 7971.
4. Mathews, W. B.; Yoo, S. E.; Lee, S. H.; Scheffel, U.; Rauseo, P. A.; Zober, T. G.; Gocco, G.; Sandberg, K.; Ravert, H. T.; Dannals, R. F.; Szabo, Z. *Nucl. Med. Biol.* **2004**, *31*, 571.
5. *Pharmaceutical Manufacturing Handbook: Production and Processes*; Gad, S. C., Ed.; Wiley: New Jersey, 2008.
6. Tai, Y. C.; Laforest, R. *Annu. Rev. Biomed. Eng.* **2005**, *7*, 255.
7. Carini, D. J.; Duncia, J. V.; Aldrich, P. E.; Chiu, A. T.; Johnson, A. L.; Pierce, M. E.; Price, W. A.; Santella, J. B., 3rd; Wells, G. J.; Wexler, R. R., et al. *J. Med. Chem.* **1991**, *34*, 2525.
8. Kolb, H. C.; Finn, M. G.; Sharpless, K. B. *Angew. Chem., Int. Ed* **2001**, *40*, 2004.
9. Kolb, H. C.; Sharpless, K. B. *Drug Discovery Today* **2003**, *8*, 1128.
10. Bock, V. D.; Speijer, D.; Hiemstra, H.; van Maarseveen, J. H. *Org. Biomol. Chem.* **2007**, *5*, 971.
11. Ramenda, T.; Kniess, T.; Bergman, J.; Steinbach, J.; Wuest, F. *Chem. Commun.* **2009**, 7521.
12. Marik, J.; Sutcliffe, J. L. *Tetrahedron Lett.* **2006**, *47*, 6681.
13. Vaidyanathan, G.; White, B. J.; Zalutsky, M. R. *Curr. Radiopharm.* **2009**, *2*, 63.
14. E.J.J. Grabowski, A.S. Thompson, Converting an alcohol to an azide with S.sub.N 2 inversion using a phosphoryl azide, Google Patents, 1995.
15. Kuhnast, B.; Hinnen, F.; Tavitian, B.; Dolle, F. *J. Labelled Compd. Radiopharm.* **2008**, *51*, 336.
16. Valdivia, A. C.; Estrada, M.; Hadizad, T.; Stewart, D.; Beanlands, R. S.; DaSilva, J. N. *J. Labelled Compd. Radiopharm.* **2012**, *55*, 57.
17. Zhou, J.; Ernsberger, P.; Douglas, J. G. *Hypertension* **1993**, *21*, 1035.
18. Kubo, Y.; Reuveny, E.; Slesinger, P. A.; Jan, Y. N.; Jan, L. Y. *Nature* **1993**, *364*, 802.
19. Zober, T. G.; Mathews, W. B.; Seckin, E.; Yoo, S. E.; Hilton, J.; Xia, J.; Sandberg, K.; Ravert, H. T.; Dannals, R. F.; Szabo, Z. *Nucl. Med. Biol.* **2006**, *33*, 5.
20. Logan, J.; Fowler, J. S.; Volkow, N. D.; Wolf, A. P.; Dewey, S. L.; Schlyer, D. J.; MacGregor, R. R.; Hitzemann, R.; Bendriem, B.; Gatley, S. J.; Christman, D. R. *J. Cereb. Blood Flow Metab.* **1990**, *10*, 740.
21. Kenk, M.; Greene, M.; Lortie, M.; Dekemp, R. A.; Beanlands, R. S.; Dasilva, J. N. *Nucl. Med. Biol.* **2008**, *35*, 515.